The 5th European sCO2 Conference for Energy Systems
March 14-16, 2023, Prague, Czech Republic

2023-sCO2.eu-147

A METHODOLOGY TO DESIGN AIR-COOLED CONDENSERS FOR SUPERCRITICAL POWER CYCLES USING CARBON DIOXIDE AND CARBON DIOXIDE MIXTURES

Pablo Rodríguez-de Arriba
Department of Energy Engineering,
University of Seville
Seville, Spain
Email: prdearriba@us.es

Francesco Crespi*
Department of Energy Engineering,
University of Seville
Seville, Spain
Email: crespi@us.es

David Sánchez
Department of Energy Engineering,
University of Seville
Seville, Spain
Email: ds@us.es

Antonio Muñoz
Department of Energy Engineering,
University of Seville
Seville, Spain
Email: ambl@us.es

ABSTRACT

The SCARABEUS project investigates the use of CO_2–based mixtures as working fluid in power cycles for next-generation Concentrated Solar Power plants. These fluids exhibit a critical temperature higher than pure CO_2, enabling dry condensation of the working fluid even at the high ambient temperatures typical of sites with a high solar radiation. As a consequence, the SCARABEUS power cycle achieves higher thermal efficiency than standard sCO_2 cycles, whose performance deteriorates significantly with ambient temperature. In any case, the actual feasibility of this concept is still to be confirmed by a complete techno-economic assessment. To that purpose, it is critical to accurately estimate the power consumption of the Heat Rejection Unit (HRU), which is one of the most important parasitic loads of the system.

Bearing all this in mind, this manuscript presents the design of a horizontal, direct air-cooled condenser (ACC). The bundle geometry proposed is comprised of seven tubes in three passes, with a staggered arrangement. The complete thermal model, developed in MatLab, has been already disclosed by the SCARABEUS consortium in a previous paper, and validated both experimentally in a dedicated test rig and against results obtained by the commercial software Xace®. The novelty in the present manuscript lies in the integration of this thermal model of the tubes with a complete design and integration tool of the whole heat rejection sub-system, including the design of a rotor-only axial fan and supporting frame. The impact of several design parameters (i.e., air temperature rise, acceptable hot pressure drops, tube length) is studied, taking into account auxiliary power consumption, footprint and cycle efficiency as main figures of merit. Two candidate mixtures are taken into account, identified in previous works by the same authors ($85\%CO_2$-$15\%C_6F_6$ and $80\%CO_2$-$20\%SO_2$), and a pure sCO_2 case is also considered for the sake of comparison. The results show that, for a given gross cycle output, using pure sCO_2 yields the smallest ACC with the lowest fan power consumption. Moreover, tube length and air face velocity are found to be the key-parameters driving the design process of an ACC, for which increasing tube length is always beneficial as far as the ACC design is concerned. Finally, various considerations regarding the role played by the optimum design of the ACC within the global optimisation of the power plant are made. It is found that the rationale employed for the design of the ACC may be in conflict with that used from an overall plant optimisation standpoint. It is hence concluded that the definition of the optimal design space of an Air-cooled Heat Exchanger (ACHE) must be included in the global optimisation of the power plant.

INTRODUCTION

Concentrated Solar Power (CSP) plants are expected to play a key role in the decarbonisation of the power generation sector. Nevertheless, as of today and despite dispatchability of CSP being a major advantage over photovoltaics and wind, the former is still far from being cost-effective due to the high LCoE [1]. This poses a need for further investigation in order to increase the solar-to-electric efficiency of this technology (hence smaller solar fields) and to reduce the overall capital cost of CSP plants, thus making it more feasible from an economic standpoint [2]. One possible solution to accomplish this objective, which is being widely investigated in literature, is to raise turbine inlet temperature up to 700-800ºC, a value significantly higher than the state-of-the-art power plants, currently operating at ~550ºC

* corresponding author(s)

DOI: 10.17185/duepublico/77329

[2]. Nevertheless, this implies overcoming several technological challenges, from the development of improved designs of both solar receivers and Thermal Energy Storage (TES) systems [3,4], to the identification of thermally stable heat transfer fluid able to operate at such high temperatures [5]; in addition to these, the development of power cycles able to take full advantage of these very high temperatures is also of primary interest. In this latter regard, supercritical CO_2 power cycles are being extensively studied, due to their noteworthy features such as higher thermal efficiency, smaller footprint and lower cycle complexity than steam-based Rankine cycles, among others. Nevertheless, at high ambient temperatures (>35ºC), usual in semi-arid locations with high solar irradiance, sCO_2 cycles experience an important efficiency drop due to the compression process being performed far from the critical point (31ºC, 73.8 bar).

To find a solution to this problem, the SCARABEUS project is currently investigating the addition of specific dopants/additives to produce a mixture with CO_2 which can be used as the working fluid in a power cycle [6]. These innovative working fluids exhibit higher critical temperatures than CO_2, which enables fluid condensation at higher. This SCARABEUS concept has already been demonstrated thermodynamically, confirming that thermal efficiencies of around 50% with minimum cycle temperatures as high as 50ºC can be achieved [7-9].

In addition to enabling higher efficiencies in sites with high ambient temperatures, the SCARABEUS concept also paves the way for the utilisation of dry cooling, which yields additional advantages in terms of reduced water consumption at reasonable auxiliary power demand. Indeed, dry cooling systems usually lead to high auxiliary power consumption (fan motors) which can potentially offset the theoretical thermodynamic advantage of advanced cycles like sCO_2 or others. Therefore, it is of utmost importance to demonstrate the technical and economic feasibility of SCARABEUS concept from a net (global) standpoint. To this end, the development of specific tools for the design and simulation of major and balance of plant (BoP) components is crucial, in particular the accurate estimate of the required heat exchange area and its auxiliary power consumption.

Modular air-cooled condensers incorporating multiple unitary cells with the same design are currently employed in CSP plants based on steam turbines (e.g., Ivanpah Solar Power Plant [10]). Each cell is typically composed of inclined finned tubes in an A-frame structure, with cooling air being forced upwards by motor-driven axial fans. For sCO_2 power cycles though, the identification of the most suitable technology for dry air cooling is not trivial, as credited by the different options considered in literature so far. Compact diffusion-bonded counter-current heat exchangers were initially studied by Moisseytsev & Sienicki [11], concluding that dry air cooling was cost-prohibitive in comparison with water cooling. Later, Moisseytsev *et al.* [12] provided a comparative analysis of two existing technologies: a modular finned tube air cooler and a compact diffusion-bonded cross-flow heat exchanger. The former was found to be the most interesting solution for dry cooling in sCO_2 cycles, yielding six times lower investment costs than if Printed Circuit Heat Exchangers (PCHE) were used, for the same power consumption.

Later studies have investigated other dry air cooling technologies. Ehsan *et al.* [13,14] investigated dry natural draft cooling towers in both direct and indirect configuration, employing an intermediate water-to-sCO_2 shell-and-tube precooler in the second case. This concept reduces the operating cost significantly but, as the investment costs of a dry natural draft cooling tower are also higher than those of a mechanical draft air cooler, a techno-economic study to assess the actual feasibility of this design is still needed. Finally, Pidaparti *et al.* [15] studied four different cooling technologies: force-draft wet indirect cooling towers, indirect dry air cooling in finned tube heat exchanger, V-shape direct air coolers and direct adiabatic cooling. For drier and hotter locations, the adiabatic cooling is seen to perform better in terms of plant efficiency and LCoE than direct dry cooling [16], though this is at the expense of a significantly higher water consumption.

The aforelisted past works refer to cycles using pure Carbon Dioxide and there are virtually no references in literature on the design of air-cooled condensers for sCO_2 mixtures. A first investigation was carried out by Illyés *et al.* [17] in the framework of SCARABEUS project. That work presents a finite-volume thermal model for the design of the pipe bundling of a finned tube ACC, validated against data provided by Kelvion Thermal Solutions, a commercial partner of the consortium.

With this in mind, the present manuscript takes this research path a step further with the aim to extend the model carried out by Illyés *et al*. to the detailed design of a modular air-cooled condenser for a 100MW (gross) CSP plant. To this end, the same tube bundling proposed in [17] is considered and, then, modules for the design and assembly of the cooling fans are developed. Two mixtures are taken into account, based on past works by the authors: Hexafluorobenzene (C_6F_6) [7] and Sulphur Dioxide (SO_2) [8]. Moreover, a pure-sCO_2 air cooler is also designed, for the sake of comparison, employing the same overall configuration of the heat rejection unit.

In the first part of the manuscript, the impact of several design variables is studied in order to find the design yielding the best balance between fan power, overall footprint, bay length and cycle efficiency. A series of Pareto fronts are produced for a set value of total-to-static fan efficiency, identifying the best ACHE design parameters for each working fluid considered. In the second part, various fan designs are produced, in order to assess the impact of incorporating case specific fan efficiencies into the previous analysis (impact on Pareto fronts). As a conclusion, and based on the results obtained. a series of considerations and suggestions are provided in order to define the best engineering practice to design ACCs for CO_2-based power cycles.

COMPUTATIONAL ENVIRONMENT

Working Fluid and Thermodynamic Cycle Models

In order to define the boundary conditions for the design of the Air-Cooled Condenser, three different combinations of cycle layout and working fluid composition are considered: Precompression cycle with 85%CO_2-15%C_6F_6 (molar fractions),

DOI: 10.17185/duepublico/77329

Recompression cycle with 80%CO_2-20%SO_2 and Recompression cycle with pure sCO_2. The layouts temperature-entropy diagrams of these cycles are provided in Figure 1.

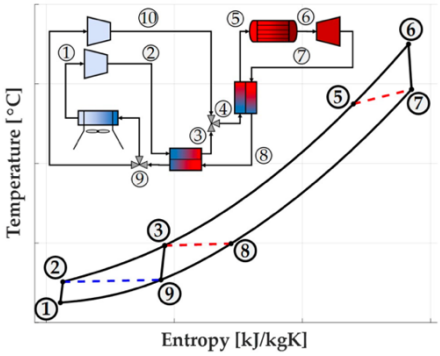

(a) Recompression with pure sCO_2 (supercritical)

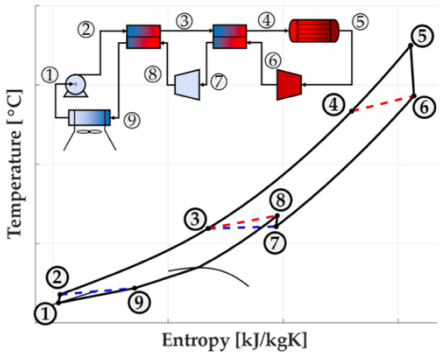

(b) Precompression with 85%CO_2-15%C_6F_6 (transcritical)

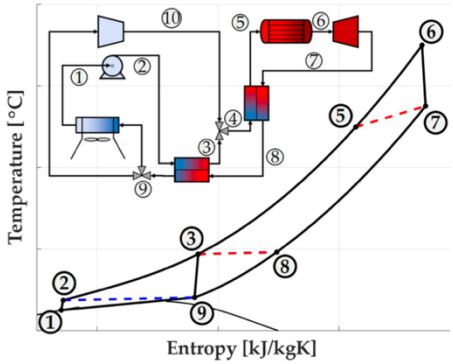

(c) Recompression cycle with 80%CO_2-20%SO_2 (transcritical)

Figure 1: Cycle layouts considered for pure (a) and blended (b,c) CO_2 systems (adapted from [9])

The first two configurations are representative of the SCARABEUS concept and have already been studied by the authors in previous publications [7,8], while the Recompression cycle is possibly the most studied configuration for sCO_2 technology, in particular for CSP applications [18]. The power cycles have been modelled using Thermoflex v.30, a commercial software by Thermoflow Inc [19], with the necessary user-defined-modules to enable simulation of SCARABEUS-specific components and features. Since these power cycles are employed to define the boundary conditions of the ACC only, a detailed description of the models falls out of the scope of this work; interested readers are therefore directed to references [7,8] where all the information of interest can be found. Table 1 presents a summary of the main features of these three cycle layouts, together with the boundary conditions to be employed in the ACC design model. It is to note that although a 1% pressure drop has initially been considered for the reference heat rejection unit during the simulations of the power cycles, the impact of this parameter on cycle performance and air-cooled condenser design is also assessed later in this work.

Table 1. Main features of different power cycle technologies and HRU boundary conditions.

	CO_2-C_6F_6	CO_2-SO_2	Pure CO_2
Layout	Precompr.	Recompr.	Recompr.
Common param.	*TIT*=700ºC, *Wel* = 100 MW (gross)		
η_{th} [%]	50.4	51.3	49.7
Q_{cond} [MW]	101	95.7	102.1
$\dot{m}_{wf}$ [kg/s]	880	516	752
$T_{wf,in}$ [ºC]	87.1	81.1	107
$T_{wf,out}$ [ºC]	50	50	50
$P_{wf,out}$ [bar]	77.8	79.1	102
$P_{wf,in}$ [bar]	Calculated from pressure drops		

The thermo-physical properties of the mixtures have been calculated with the commercial software Aspen Plus v12 [20] and embedded in Thermoflex by means of look-up tables. A thorough description of the two dopants hereby considered, C_6F_6 and SO_2, can be found in previous works by the authors, together with a discussion of their safety hazards according to NFPA704 standard. The main specifications needed to obtain the thermo-physical properties, including the specific equation of state used and the corresponding binary interaction parameters, are summarised in Table 2. Attention must be paid to transport properties (i.e. thermal conductivity and dynamic viscosity), for which limited information is found in literature. Refprop10 includes a calculation model for pure CO_2 and for CO_2-SO_2 mixtures, which is employed in the present [21]. On the other hand, only very limited information is available for CO_2-C_6F_6 mixtures; in fact, the SCARABEUS consortium is currently undertaking experimental activity in order to calibrate a suitable model to estimate transport properties of this fluid, based on the SUPERTRAPP methodology. The results of this investigation will be disclosed in the coming months by other partners of the SCARABEUS consortium. Thus, due to the lack of available data, the TRAPP predictive model as calculated by Aspen Plus v12 has been used in this work.

DOI: 10.17185/duepublico/77329

Table 2. Specifications of working fluids

	85%CO_2 15%C_6F_6 (v)	80%CO_2 20%SO_2 (v)	Pure sCO_2
T_{cr} [ºC]	102.1	64.2	31
P_{cr} [bar]	121.3	91.85	73.8
EoS	Peng-Robinson	PC-SAFT	Span & Wagner
Kij	$0.16297 - 0.0003951 \cdot T$	0.0121	-
Transport prop.s method	TRAPP	REFPROP 10	REFPROP 10

Finned Tube Heat Exchanger Model

The Heat Rejection Unit design model presented in this work is an ACC based on a finned-tube heat exchanger. Similarly to the original configuration proposed by Moisseytsev in [12], the working fluid flows inside horizontal tubes, whose thermal performance is enhanced by the addition of circular fins. Nevertheless, rather than considering a fully horizontal layout as in [12], the tubes are here arranged in three vertical passes, with a staggered distribution. Thus, the air flows upwards, driven by axial fans, and across seven rows of tubes, distributed in three different passes. The hot fluid flow on the inside enters from the upper part of the ACC and is split in three tubes, constituting the first pass of the bundle. The second pass is also composed of three tubes, whilst the flow is mixed in a single tube in the final pass. This tube bundling, presented in [17] originally, is selected in order to reduce pressure drops on the hot fluid side. The tubes at the end of each pass discharge into a header, where the fluid is mixed so that its conditions are homogeneous at the inlet to the next pass. A graphical representation of the aforedescribed heat exchanger is provided in Figure 2, whilst Table 3 provides the main characteristics of the tubes and fins.

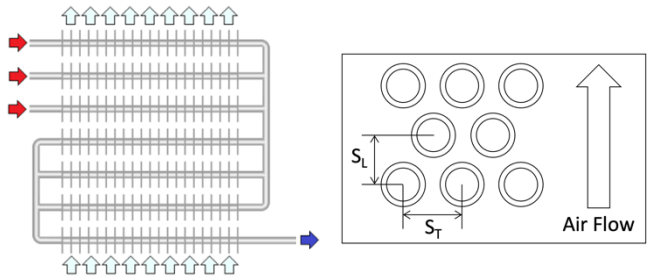

Figure 2: Tube geometry and bundling staggered arrangement (adapted from [17])

The finned tube heat exchanger has been modelled in MATLAB. Following the work by Shah & Sekulic [22], each row is discretized in several sub-heat exchangers (sub-HX), in order to reduce the impact of the high variation of thermo-physical properties of the working fluid (constant fluid properties in each sub-HX can hence be used). The number of sub-HX is set to 50 after a specific sensitivity analysis, a number found to be a good compromise between numerical consistency and computational burden.

Table 3. Specifications of reference tube bank and fins (ACC)

Parameter	Value
Tube internal / external diameter	20.76 mm / 26.8 mm
Transversal / Longitudinal pitch	66.7 mm / 57.7 mm
Tube material	Carbon Steel
Fin type	Circular fins
Fin material	Aluminium 1100-annealed
Fin height / thickness / spacing	15.9 mm / 120μm / 2.52 mm
# tubes per row	7
# passes / # tubes per pass	3 / 3-3-1
Tube bundle arrangement	Staggered
Fan draft type	Induced

Definitions for the geometry of tube-fin heat exchangers can be found in [22] whilst fin efficiency of circular fins is computed according to the information in [23]. The condensation heat transfer coefficient of the SCARABEUS mixtures is computed by means of Cavallini's model [24], as suggested in [17], which is also valid for zeotropic mixtures as it is the case for the working fluids in SCARABEUS. For the cooling of sCO_2, the correlation by Krasnoshchekov and Protopopov [25] is recommended in literature to estimate heat transfer near the critical point [26]. The air-side convective coefficient is calculated using Briggs & Young's correlation as suggested in [22] for finned tubes. Finally, the fouling factors are set to 0.00176 $m^2 \cdot K/W$ on both sides [27]. Each sub-HX can be treated as a cross-flow heat exchanger, where both fluids remain unmixed. The effectiveness-NTU functions for such configuration are reported in [23].

Estimating pressure drop on both sides accurately is crucial in the design of an ACHE. The pressure drop on the inner side (working fluid) has a negative influence on the thermal efficiency of the power block whereas the pressure drop on the air side brings about a higher auxiliary power consumption and, accordingly, lower net plant efficiency. The model by Del Col *et al*. [28] is recommended in [17] for the calculation of pressure drops during condensation of the SCARABEUS mixtures. For sCO_2, Colebrook's correlation modified by the property ratio method, as explained in [29](Chap.8), is implemented to account for property variations between the fluids near the wall and the bulk fluid. For the air-side pressure drop, Robinson and Briggs' correlation is employed for circular finned tubes [22,30], and an additional 20% of the bundle pressure drop is added to account for other sources of friction loss as explained in [22].

The heat transfer model of the finned tube heat exchanger is solved by starting from the hot end. A priori, only the air temperature distribution at the inlet (lower row) is known, as this is assumed uniform and equal to ambient temperature. On the other hand, the mean value of air temperature at outlet can be defined by means of an energy balance, but not its distribution along the length of the pass. Therefore, the heat exchange must be solved through an iterative procedure, guessing an initial outlet air temperature distribution and converging the inlet distribution which can be computed by solving the aforedescribed model.

DOI: 10.17185/duepublico/77329

The design of the ACHE requires the user to specify the thermodynamic state at the inlet and the outlet of both the hot fluid and air, as well as a target hot side pressure drop. From these specifications, the number of tubes and the length of the pass are determined. A flowchart of the ACHE design tool is depicted in Figure 3.

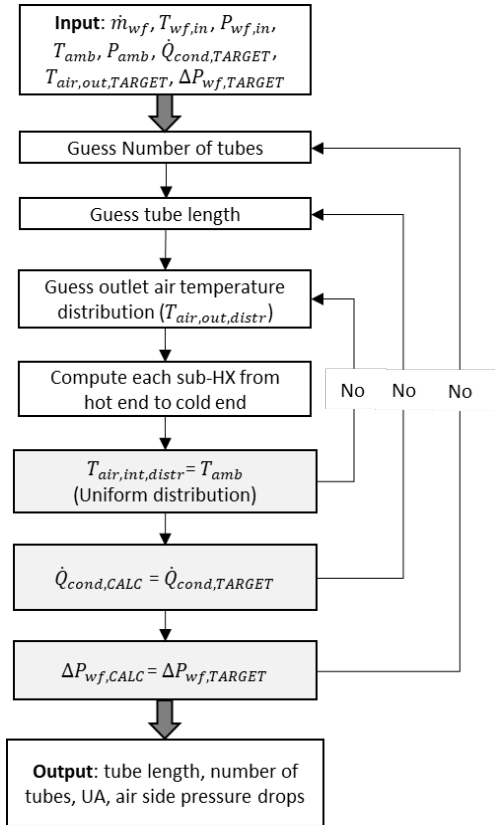

Figure 3: Flow chart of ACHE design code

AXIAL FAN MODEL

A numerical tool capable of producing a preliminary design of a (single-rotor, no stator) axial fan and of estimating its total-to-static efficiency has been implemented, based on the work by Wilkinson [31]. In order to produce the fan design, a number of specifications such as fan diameter (D_{fan}), air flow rate, total-to-static pressure, blade tip speed, inlet temperature and inlet pressure are needed. Blade tip speed is set to 58 m/s, according to Wilkinson's work, whilst the other parameters are optimised for each case, depending on the working fluid and on the performance required from the fan. The hub-to-tip ratio is estimated using the model developed by Bruneau [32]. The exit axial and swirl velocities are computed by means of an optimisation procedure with the aim to minimise the kinetic energy flux as described in Von Backström [33]. Finally, the chord length distribution is computed as explained in Bruneau [32], assuming a reference airfoil (NASA-LS-0413, in the present work). With this information, the total-to-total and total-to-static efficiencies are computed.

AIR-COOLED HEAT EXCHANGER MODEL

The entire set of tubes is divided into independent units (bays), constituting the ACHE module represented in Figure 4. Due to the large length of the tubes, each bay is typically equipped with more than one axial fans, which can be of either the forced or induced draft type. The bay face area and the plenum height are linked to the fan casing area in order to ensure a good air distribution across the tube bundle [34]. The plenum height is set to $0.3 \cdot D_{fan}$, following best engineering practice [34], and a minimum threshold of the ratio between fan area and bay face area is set to 40% [30]. Additionally, in this work, the projected face area covered by each fan is set to $1.5 \cdot D_{fan}$ in the longitudinal direction of the bay and $1.2 \cdot D_{fan}$ in the transversal direction. This yields a fan-area-to-tube-bundle-face-area ratio of 43.6%, which is aligned with the aforementioned common engineering practice. It is worth noting that these reference values and constraints have been set in this work according to common engineering practice, but they will be subject to techno-economic optimisation in future, according to the scope of activities in SCARABEUS.

Under these assumptions, the total number of fans, the number of bays and the number of tubes per bay are calculated and then rounded up to the nearest integer in all cases.

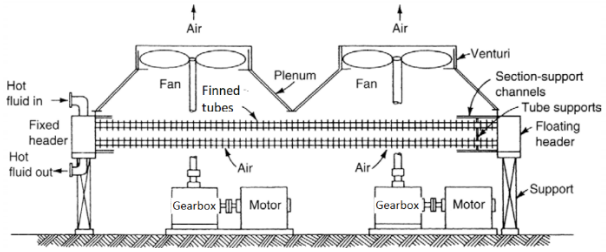

Figure 4: General scheme of an induced draft ACHE [Adapted from 30]

MODELS VALIDATION

The finned-tube heat exchanger model has been validated against three different designs presented in [17]: a 92%CO_2-8%C_6F_6 blend, with both simple and enhanced tubes, and pure CO_2 with enhanced tubes[1]. The heat exchanger has been designed imposing the same heat duty, the same target inner pressure drop and the same air temperature rise. The results are compared in terms of external HX area (A_{HX}), pass length, number of tubes and Overall Heat Transfer Coefficient (U). The results of this validation are provided in Table 4.

[1] The enhanced configuration corresponds to corrugated surfaces both inside the tubes and in the fins on the air side, as thoroughly explained in [17]. The specifications of this enhanced configuration are confidential, proprietary of Kelvion Thermal Solutions, and cannot be disclosed here. For the sake of accessibility of this study, authors decided to employ the simple configuration in the design of the ACC. The enhanced configuration has been considered in the validation of the tool only.

DOI: 10.17185/duepublico/77329

Table 4. Specifications of reference tube bank and fins (ACC)

Working Fluid (WF)	**CO_2-C_6F_6**			**CO_2-C_6F_6**			**Pure CO_2**		
Enhanced	No			Yes			Yes		
Q_{cond} [MW]	236								
$\dot{m}_{wf}$ [kg/s]	1200			1200			1749		
$P_{wf,in}$ [bar]	92			92			100		
WF temperatures	114ºC to 51ºC								
ΔP_{wf} [bar]	0.46								
Air temperatures	36ºC to 59.5 ºC			36ºC to 63.1 ºC			36ºC to 65.4 ºC		
	This work	Illyés *et al.* [17]	Δ [%]	This work	Illyés *et al.* [17]	Δ [%]	This work	Illyés *et al* [17]	Δ [%]
A_{HX} [m^2]	481135	487800	-1.37	412990	417300	-1.03	390412	381700	2.28
L_{tube} [m]	20.85	19.30	8.04	15.92	14.90	6.81	10.15	10	1.49
# tubes	1858	2030	-8.47	2091	2250	-7.07	3100	3055	1.47
U [W/m2K]	21.93	23.00	-4.67	27.35	28.80	-5.05	28.75	28.6	0.52

The total (external) heat exchange area shows very good agreement in all three cases, with relative deviations in the order of 1% for CO_2-C_6F_6 blends and slightly above 2% for the pure sCO_2 case; this latter difference could be explained by the different correlation used to estimate the sCO_2 heat transfer coefficient. As previously commented, Krasnoshchekov and Protopopov's correlation is used in this work instead of Gnielinski's (employed in [17]), given that the former is more adequate to predict the behaviour of CO_2 near the critical point [26].

Good match is also found for the estimated tube characteristics (length and number), with relative deviations below 1.5% when pure CO_2 is considered. On the contrary, a larger deviation is observed for these parameters when using CO_2-C_6F_6, in the order of 8%. This is caused by the different transport properties considered (Illyés *et al.* employed preliminary results obtained with SUPERTRAPP) and, to a lesser extent, by fin efficiency. In this regard, this parameter is set to the constant value of 77.5% in [17], whilst it is calculated for each case in the present work, yielding values around 65.5% for the boundary conditions presented in Table 4. It is worth noting that, for a given heat duty, length and number of tubes present inversely proportional trends (i.e., reducing the length poses the need for a higher number of tubes, and vice versa). Thus, all the possible combinations of these two parameters yield very similar total A_{HX}. This highlights the need to reduce the uncertainty introduced by transport properties of the working fluid, a task which is currently being undertaken within the SCARABEUS consortium.

On the other hand, the axial fan design tool has been validated against the case study from [31]. The fan design tool has been validated for the reference case defined in Table 3.2 from [31]. Relative deviations of both total-to-static efficiency and hub-to-tip ratio are lower than 1%.

DISCUSSION OF RESULTS

PRELIMINARY CONSIDERATIONS REGARDING ACHE DESIGN

Once the capacity of the condenser to actually reject the amount of thermal energy that is needed to produced saturated liquid at the outlet is verified, it is the time to assess other techno-economic features of this component: size (total volume occupied by the bundles, V_{HX}), fan power (W_{fan}) and pressure drop on the inner side of the tubes (ΔP_{wf}). The first two parameters are linked to the design of the ACHE only and do not have any impact on the thermal performance of the power cycle. On the contrary, cycle efficiency is sensitive to ΔP_{wf}, which has an impact on the global optimisation of the SCARABEUS system. This global optimisation is out of the scope of this paper though, which introduces a methodology to design the HRU only, and hence only trade-offs between component size and power consumption are studied here. Some high-level considerations about the impact on cycle performance will nevertheless be given in the concluding section of the paper. The total volume occupied by the tube bundles (see Equation 1) is proportional to the product of tube length (L_{tube}) and number of tubes in parallel (N_{tubes}), given that the number of rows is set to seven and the longitudinal and transversal pitches are those indicated in Table 3.

$$V_{HX} = L_{tube} \cdot N_{tubes} \cdot S_L \cdot N_{rows} \cdot S_T \quad (1)$$

Fan power consumption is calculated as the product of volumetric air flow rate ($\dot{V}_{air}$) and the pressure drops across the bundle (ΔP_{air}) divided by fan total-to-static efficiency (η_{TS}), as shown in Equation 2. It is to note that, in this section, η_{TS} is set to 68%, an assumption that will be revised in a later section.

$$\dot{W}_{fan} = \dot{V}_{air} \cdot \Delta P_{air} / \eta_{TS} \quad (2)$$

DOI: 10.17185/duepublico/77329

With the geometrical specifications of the tubes (including D_{fan}) and fins set to the values indicated in Table 3, the design code for the finned-tube heat exchanger presents two degrees of freedom: the temperature rise experienced by the air stream (ΔT_{air}) and target ΔP_{wf}. The first parameter is inversely proportional to the volumetric air flow rate circulating across the heat exchanger. The second parameter directly affects the number of tubes in parallel constituting the bundling, for a given tube diameter: lower pressure drops imply a higher number of tubes (reduction of flow velocity).

It is worth noting that either if the inner pressure drop is reduced or if the air temperature rise is increased, the overall transfer coefficient (U) decreases as a consequence of the lowerflow velocity of both fluids (low Nusselt number); this brings
about a need for larger heat transfer areas to meet the required heat duty. Interestingly, a larger air temperature rise also brings a larger logarithmic mean temperature difference in the condenser (LMTD), which would partly offset this need (heat transfer area decreases when LMTD increases).

Regarding V_{HX}, this increases with the number of tubes in parallel and with their length (and so does the total heat transfer area), and it also increases for decreasing values of U. On the other hand, the auxiliary power consumption is strongly sensitive to the air face velocity (v_{face}), as it represents the product of $\dot{V}_{air}$ (proportional to v_{face}) and ΔP_{air} (proportional to ${v_{face}}^2$). The air face velocity is defined as the volumetric flow rate divided by the frontal area of the heat exchanger, in Equation 3, which is in turn proportional to the number of tubes and their length (thus, to V_{HX}). As a consequence, V_{HX} and $\dot{W}_{fan}$ present an opposite trend with respect to ΔT_{air} and ΔP_{wf}, since $\dot{W}_{fan}$ decreases for higher ΔT_{air} and lower ΔP_{wf}.

$$v_{face} = \dot{V}_{air}/A_{FR} = \dot{V}_{air}/(L_{tube} \cdot N_{tubes} \cdot S_T) \qquad (3)$$

Bearing all this in mind, the existence of Pareto fronts defining the design space of the ACHE is proven. In other words, the optimal design space for the ACHE (i.e., Pareto front) is formed by the designs for which a certain fan power can be achieved with the minimum heat exchanger volume or, conversely, the designs for which, given a certain heat exchanger volume, fan power is minimised.

To generate these Pareto fronts, an extensive sensitivity analysis to ΔT_{air} and ΔP_{wf} is performed for the three systems under study: Recompression cycle with CO_2-SO_2, Precompression cycle with CO_2-C_6F_6 and Recompression cycle with sCO_2. The results of this preliminary analysis are presented in Figure 5, where the overall design spaces for these systems, (i.e., the trend of $\dot{W}_{fan}$ as a function of V_{HX} for different combinations of ΔT_{air} and ΔP_{wf}) are provided. It can be observed that the best compromise between $\dot{W}_{fan}$ and V_{HX} corresponds to the pure sCO_2 case. This means, in other words, that the ACHEs designed for the two SCARABEUS mixtures always present higher $\dot{W}_{fan}$ than the pure CO_2 case for a given V_{HX}, or higher V_{HX} for given $\dot{W}_{fan}$. This is probably due to the higher working fluid temperature at the inlet to the HRU in the pure sCO_2 case (see $T_{wf,in}$ in Table 1), and presents a twofold explanation: i) LMTD is increased, reducing the total heat transfer area needed (and V_{HX}); ii) higher $T_{wf,in}$ also leads to higher ΔT_{air}, which in turn reduces $\dot{V}_{air}$ and, consequently, $\dot{W}_{fan}$. Finally, it is noted that this could also be caused by the characteristics of the condensation of zeotropic mixtures. This is nevertheless, beyond the scope of the present manuscript and will be addressed in future works.

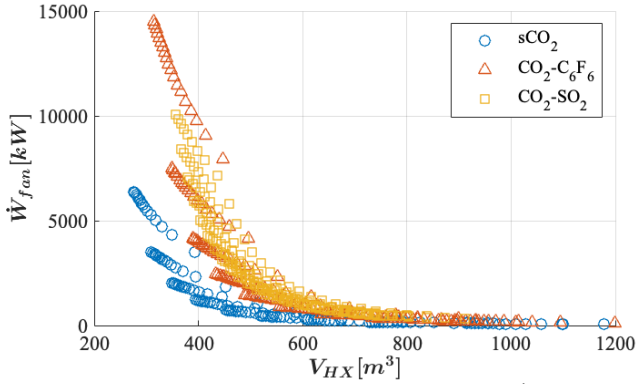

Figure 5: Overall design spaces based on $\dot{W}_{fan}$ and V_{HX}, considering the three different systems under analysis.

Identification of Key Parameters for ACHE Design

Apart from these considerations, another key parameter in the design of the ACHE is the maximum allowable tube length, which influences both mechanical integrity and economic feasibility of this component. Two conditions can lead to higher L_{tube}: higher ΔP_{wf} (a reduction in the number of tubes needs to be balanced by longer lengths to yield similar heat transfer area) and higher ΔT_{air} (due to the reduced overall heat transfer coefficient). As a consequence, it is clear that the Pareto front is obtained where either ΔT_{air} or ΔP_{wf} take highest values, compliant with the constraint on maximum tube length.

The impact of considering different maximum L_{tube} is now studied. For the sake of simplicity, this discussion is limited to the CO_2-SO_2 case, but the results are representative of the other two systems. Figure 6 highlights the points of the previous sensitivity analysis where tube length is set to 12, 15, 18 and 22 m respectively. It is worth noting that additional simulations have been done for this analysis, hence some of the new points fall outside of the original overall design space of Figure 5 (represented by light grey square markers in Figure 6). First and foremost, it is observed that the highlighted points constitute different Pareto fronts. This is not a trivial conclusion, and it means that the optimal design spaces are actually driven by L_{tube}, and that longer tubes are always preferred in terms of either V_{HX} and $\dot{W}_{fan}$. Nevertheless, it is also observed that the Pareto fronts tend to converge if L_{tube} is increased, with the yellow square markers (18m tubes) being very close to the red triangle (22m). This means that, even if from a purely theoretical standpoint, a higher L_{tube} is always beneficial, exceeding 18m does not provide any practical improvement from an engineering standpoint. Bearing this in mind, L_{tube} is proven to be a key-parameter for ACHE design.

DOI: 10.17185/duepublico/77329

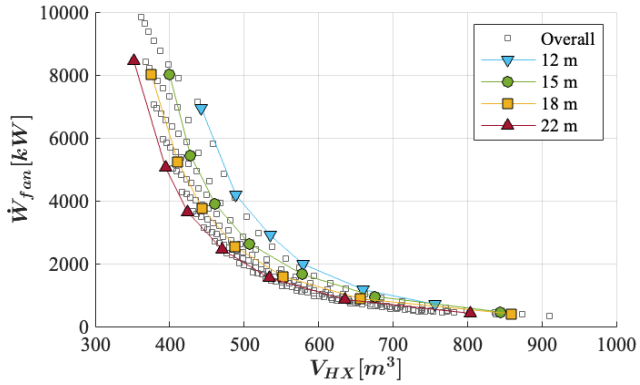

Figure 6: Overall design space for CO_2-SO_2 system. Pareto fronts obtained setting L_{tube} of 12, 15, 18 and 22 m are highlighted.

A further step would be to identify a variable capable of unequivocally defining a given point of the Pareto front, which can also maintain this feature independently from the working fluid taken into account, hence affecting the three systems considered similarly. Such parameter seems to be the v_{face} which, indeed, is proportional to the cube root of fan power to heat exchanger volume ratio, multiplied by a constant that depends on air properties and fan efficiency. As η_{TS} is considered constant in this section and air properties hardly change for the temperature variations in the design space, the correlation between v_{face} and $(\dot{W}_{fan}/V_{HX})^{1/3}$ is perfectly linear (see Figure 7). With all this in mind, it can be concluded that the optimal design space of an ACHE should be defined in terms of tube length and air v_{face}, rather than ΔT_{air} and ΔP_{wf}.

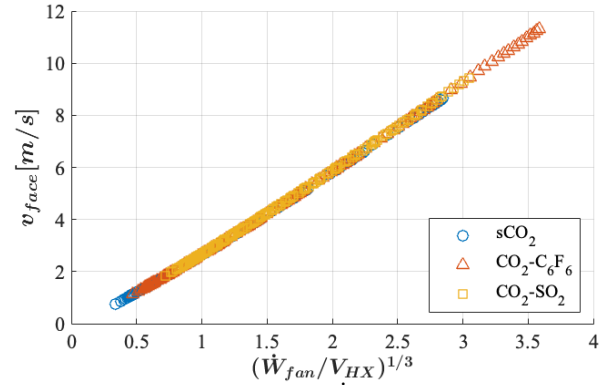

Figure 7: v_{face} as a function on $\dot{W}_{fan}$ to V_{HX} ratio.

Impact of Fan Design

The previous analysis was developed under the assumption of constant fan total-to-static efficiency for the sake of simplicity. Nevertheless, this does not necessarily hold true for all points explored during the sensitivity analysis, since they correspond to different fan design conditions (different flow rate and different required pressure rise). To test the validity of the hypothesis, several points of the Pareto front corresponding to a tube length of 18m are collected and an axial fan is designed for each one of them. These points are defined by a v_{face}, as explained before. Fan diameter is set to 5.18 m (17 ft), and an induced draft configuration is chosen in order to reduce hot air recirculation [30]. Results are provided in Table 5.

Table 5. Fan η_{TS} as a function of v_{face}. Results obtained with in-house fan design model.

v_{face} [m/s]	sCO_2	CO_2-C_6F_6	CO_2-SO_2
2	65.0%	64.9%	65.8%
3	68.1%	68.7%	68.6%
4	67.2%	68.7%	66.9%
5	64.0%	62.4%	62.9%
6	62.8%	59.4%	59.9%

Observing the results provided in Table 5, it is found that a fan efficiency of 68% is a good assumption for v_{face} in the 3-4 m/s range. At lower values, the tip speed needs to be reduced below that of the maximum allowable (58m/s) in order to find a suitable solution, penalising efficiency. At higher v_{face}, fan performance deteriorates importantly and η_{TS} falls below 64%.

Best Engineering Practice and Final Considerations

This section introduces some basic design guidelines gathered from ACHE handbooks. Maximum tube length is usually limited by either manufacturing, transportation or plant layout constraints. The horizontal ACHE studied in Moisseytsev [12], taken from a vendor quote, has a tube length of 18.6 m (61 ft), what is consistent with catalogues from other manufacturers. According to Kakaç, tube length is ultimately limited to 30 m by transportation [27]. Regarding bundle width, Serth claims it to be limited to a maximum of 4.3 m (14 ft) due to transportation constraints [30], but several bundles can be placed together within the same ACHE bay. This same author recommends v_{face} between 2 and 4 m/s to achieve a good trade-off between air side pressure drop and external heat transfer coefficient [30]. This set of common practises is in line with the results presented in this paper; therefore, a reference ACHE design for the three systems is proposed by setting tube length to 18 m and v_{face} to 3 m/s. The results are presented in Table 6.

Table 6. Reference bay design

	sCO_2	CO_2-C_6F_6	CO_2-SO_2
L_{tube} [m]	18	18	18
v_{face} [m/s]	3	3	3
ΔP_{wf} [bar]	0.81	0.51	0.16
ΔT_{air} [ºC]	24.9	19.8	17.1
D_{fan} [m]	5.18	5.18	5.18
η_{TS} [%]	68.1	68.7	68.6
Fan arrangement	Induced	Induced	Induced
U [W/m^{2}K]	23.58	21.5	21.4
A_{HX} [m^2]	222480	278160	304880
Pinch point [ºC]	9.48	9.88	9.2
# bays	11	14	15
# fans per bay	3	3	3
N_{tubes}	90	89	91
V_{HX} [m^3]	481	601	660
$\dot{W}_{fan}$ [kW]	678	812	872

DOI: 10.17185/duepublico/77329

Figure 8 plots the Pareto fronts for the three systems balancing heat exchanger volume and fan power for a tube length of 18 m. The aforecited recommendation in terms of v_{face} ranging from 2 to 4 m/s is added and highlighted with filled markers. The black markers for each Pareto front indicate the reference bay from Table 6.

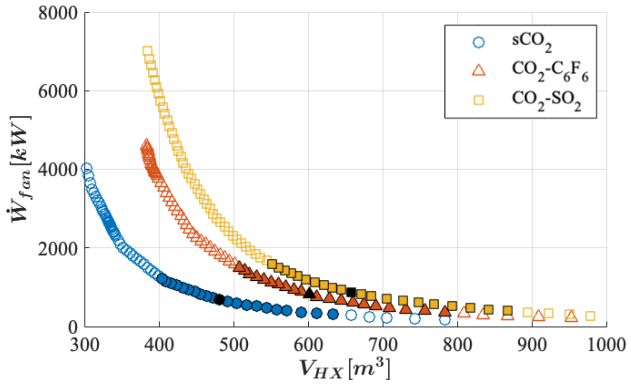

Figure 8: Pareto fronts corresponding to a tube length of 18 m. Reference bay designs are highlighted with black markers. Filled-in coloured markers correspond to v_{face} ranging 2 to 4 m/s.

According to the results in Figure 8, the optimum ACHE design stems from the best compromise between $\dot{W}_{fan}$ and V_{HX}, which is found in the left-bottom corner of the Pareto front and corresponds to high values of L_{tube}. This means that, as far as the ACHE is concerned, it is always beneficial to increase the length of the tubes. Nevertheless, even if longer tubes allow the rejection of the same heat duty with lower $\dot{W}_{fan}$ and V_{HX}, this comes at the expense of larger ΔP_{wf} (for given ΔT_{air}), which can be detrimental for cycle performance. In order to assess how much thermal efficiency is affected by changes in ΔP_{wf}, simulations are carried out with Thermoflex for the three systems in analysis. Pressure drops in the range from 0 (ideal case) to 2 bar are considered (0.46 bar being the reference value employed in [17], see Table 4), and the results are provided in Figure 9. Similar thermal efficiency drops ($\Delta\eta_{th}$) are observed for both Recompression with pure sCO_2 and transcritical Recompression with CO_2-SO_2, rounding 0.4 percentage points (pp) at 2 bar. This confirms the very similar performances obtained by these two systems, already highlighted in [8,9]. On the other hand, Precompression with CO_2-C_6F_6 shows smaller $\Delta\eta_{th}$, in the order of 0.15 pp. This is due to the further degree of optimisation that characterises this system, enabled by the addition of the precompressor (stations 7-8 in Figure 1(b)), which is capable of overcoming the limitation imposed by condensing pressure on turbine exhaust pressure (more information in [9]).

Although at first glance these performance drops look small, it is also true that they have a negative impact on the upstream component of the power plant. For instance, lower cycle efficiency implies larger aperture area (hence cost) of the solar field and also larger inventory of HTF to be pumped (hence higher cost and auxiliary power consumption).

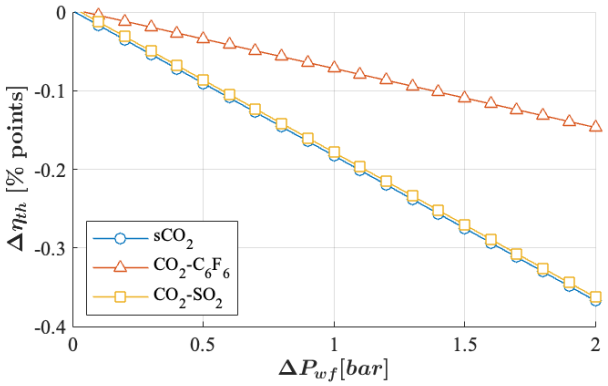

Figure 9: Thermal efficiency change as a function of internal pressure drops across the ACC, considering the three different systems under analysis.

In addition, it is to note that, for a given L_{tube}, ΔP_{wf} and ΔT_{air} exhibit opposite trends that create a counteracting effect on cycle thermal efficiency. In fact, ΔT_{air} must increase in order to reduce ΔP_{wf}. Nevertheless, if a reduction in ΔP_{wf} is beneficial for cycle efficiency, a higher ΔT_{air} leads to increasing air temperatures at ACC outlet. This latter effect could lead to higher minimum cycle temperatures with a subsequent reduction of thermal efficiency, offsetting the potentially beneficial effect of a lower ΔP_{wf}. Similarly, reducing ΔT_{air} could be beneficial for cycle efficiency (lower minimum cycle temperatures could be achieved), and this becomes even more interesting considering the possibility to tailor the composition of the mixtures to maximise cycle efficiency according to minimum cycle temperature, as discussed in [7]. In this regard, thermal efficiency gains in the order of 1 pp can be obtained when reducing cycle minimum temperature from 50ºC to 40ºC [8]. Nevertheless, for a given L_{tube}, lower ΔT_{air} would lead to higher ΔP_{wf} (lower thermal efficiency) and, following the Pareto front, to higher fan power consumption (lower net efficiency). With all of this in mind, the identification of the optimum value of L_{tube} and, generally speaking, the optimum design of the ACHE, must stem from global system global optimization rather than addressed independently in an optimization of condenser design.

Last but not least, some considerations regarding fans optimisation and their integration in the ACC are worthwhile, even if this task falls out of the scope of the present work. Generally speaking, larger fans are desirable as they enable a lower number of fans and, following the bay design guidelines presented above, also the number of bays (reduced capital cost), since multiplicity of components is usually detrimental for plant economics. However, by reducing the number of independent bays, the capacity of the system to control part-load performance effectively (i.e., off-design cooling capacity) at partial load is also compromised. Again, it is not trivial to provide a solution for this problem, which will be addressed from a techno-economic standpoint in future works by the authors also considering ACC integration and part-load operation strategies.

DOI: 10.17185/duepublico/77329

CONCLUSIONS

In this paper, a methodology to design a finned tube air-cooled condenser for pure sCO_2 and CO_2-based mixtures is presented and discussed. An in-house code for the design of axial fans is included. Three different systems are considered, identified in previous works by the authors: a transcritical precompression cycle running on $85\%CO_2$-$15\%C_6F_6$, a transcritical recompression cycle with $80\%CO_2$-$20\%SO_2$ and a supercritical sCO_2 recompression cycle. A sensitivity analysis to air temperature rise and hot pressure drop is carried out in order to obtain Pareto fronts defining the optimal design space for the ACC of the three systems under analysis.

The main outcomes of this study are as follows:

- The model presented is a specific tool developed for the design of ACCs, and it is here employed to study the effect of various design parameters.
- The optimal design of the ACC depends strongly on the working fluid considered.
- The common practice of limiting the length of the tubes to ~18.3m and air face velocity to ~4 m/s is confirmed by the results of the analysis.
- Tube length and air face velocity are found to be the two key-parameters in the design of the ACHE.
- Increasing the length of the tubes is always beneficial for ACHE design since it reduces both fan power and HX size of. Nevertheless, this also leads to higher n pressure drops on the hot side, with a detrimental effect on thermal efficiency.
- As a consequence, it cannot be concluded that the optimum ACC design, corresponding to the highest internal pressure drop, also corresponds to the optimum conditions of the overall plant. In fact, it is very likely not the case.
- In this regard, it is shown that the rationale employed for the design of the ACHE is actually the opposite to the one that should be used from a global plant optimisation standpoint, which is evidently not a trivial task.
- As a conclusion, it becomes clear that the definition of the optimal design space of an ACHE must be included in the global optimisation of the power plant.

NOMENCLATURE

A_{FR}	Tube bundling frontal area	(m^2)
A_{HX}	External Heat Exchanger area	(m^2)
ACC	Air-cooled condenser	(-)
ACHE	Air-cooled heat exchanger	(-)
CSP	Concentrated Solar Power	(-)
D_{fan}	Fan diameter	(m)
HRU	Heat Rejection Unit	(-)
HX	Heat Exchanger	(-)
LCoE	Levelised Cost of Energy	($/MWh)
LMTD	Logarithmic mean temperature difference	(K)
L_{tube}	Length of tubes	(m)
N_{rows}	Number of rows	(-)
N_{tubes}	Number of tubes	(-)
PCHE	Printed Circuit Heat Exchanger	(-)
pp	percentage points	(%)
SoA	State of the Art	(-)
S_L	Longitudinal pitch	(m)
S_T	Transversal pitch	(m)
TES	Thermal Energy Storage	(-)
TIT	Turbine Inlet Temperature	(ºC)
U	Heat transfer coefficient	(W/m^2K)
UA	Thermal conductance	(W/K)
$\dot{V}_{air}$	Air volumetric flow rate	(m^3/s)
v_{face}	Air face velocity	(m/s)
V_{HX}	Total volume of tube bundling	(m^3)
WF	Working fluid	(-)
W_{fan}	Fan power consumption	(kW)
ΔP_{air}	Air pressure drop	(Pa)
ΔP_{wf}	Workng fluid pressure drop	(Pa)
ΔT_{air}	Air temperature rise	(ºC)
η_{th}	Cycle thermal efficiency	(%)
η_{TS}	Fan total-to-static efficiency	(%)

ACKNOWLEDGEMENTS

The SCARABEUS project has received funding from the European Union's Horizon 2020 research and innovation programme under grant agreement N ° 814985. The SCARABEUS team at Kelvion Thermal Solutions is gratefully acknowledged for their valuable contribution in the definition of the operational limits and best engineering practice of the ACC.

REFERENCES

[1] IRENA (2021), Renewable Power Generation Costs in 2020, *International Renewable Energy Agency, Abu Dhabi.*

[2] He, Y. L., Qiu, Y., Wang, K., Yuan, F., Wang, W. Q., Li, M. J., & Guo, J. Q. (2020). Perspective of concentrating solar power. *Energy*, 198, 117373.

[3] Merchán, R. P., Santos, M. J., Medina, A., & Hernández, A. C. (2021). High temperature central tower plants for concentrated solar power: 2021 overview. *Renewable and Sustainable Energy Reviews*, 111828.

[4] Ho, C. K. (2017). Advances in central receivers for concentrating solar applications. *Solar energy*, 152, 38-56.

[5] Polimeni, S., Binotti, M., Moretti, L., & Manzolini, G. (2018). Comparison of sodium and KCl-MgCl2 as heat transfer fluids in CSP solar tower with sCO2 power cycles. *Solar Energy*, 162, 510-524.

[6] Supercritical CARbon dioxide Alternative fluids Blends for Efficiency Upgrade of Solar power plants. https://www.scarabeusproject.eu/. Retrieved October 24th 2022.

[7] Crespi, F., de Arriba, P. R., Sánchez, D., Ayub, A., Di Marcoberardino, G., Invernizzi, C. M., ... & Manzolini, G. (2022). Thermal efficiency gains enabled by using CO2 mixtures in supercritical power cycles. *Energy*, 238, 121899.

[8] Crespi, F., de Arriba, P. R., Sánchez, D., & Muñoz, A. (2022). Preliminary investigation on the adoption of CO2-SO2

DOI: 10.17185/duepublico/77329

working mixtures in a transcritical Recompression cycle. *Applied Thermal Engineering*, 211, 118384.
[9] Rodríguez-deArriba, P., Crespi, F., Sánchez, D., Muñoz, A. & Sánchez, T. (2022). The potential of transcritical cycles based on CO2 mixtures: An exergy-based analysis. *Renewable Energy*, vol. 199, p. 1606-1628.
[10] Ivanpah Solar Electric Generating System CSP Project. https://solarpaces.nrel.gov/project/ivanpah-solar-electric-generating-system. Retrieved October 24th 2022.
[11] Moisseytsev, A., & Sienicki, J. J. (2014). Investigation of a dry air cooling option for an S-CO2 cycle. *Proceedings of Supercritical CO2 Power Symposium, Pittsburgh (PA)*
[12] Moisseytsev, A., Lv, Q., & Sienicki, J. J. (2017). Heat Exchanger Options for Dry Air Cooling for the sCO2 Brayton Cycle, *Proceedings of ASME Turbo Expo 2017*
[13] Ehsan, M. M., Guan, Z., Klimenko, A. Y., & Wang, X. (2018). Design and comparison of direct and indirect cooling system for 25 MW solar power plant operated with supercritical CO2 cycle. *Energy conversion and management*, 168, 611-628.
[14] Ehsan, M. M., Wang, X., Guan, Z., & Klimenko, A. Y. (2018). Design and performance study of dry cooling system for 25 MW solar power plant operated with supercritical CO2 cycle. *International Journal of Thermal Sciences*, 132, 398-410.
[15] Pidaparti, S. R., White, C. W., & Weiland, N. T (2022). Cooling System Cost and Performance Models to Minimize Cost of Electricity of Direct sCO2 Power Plants. In *Proceedings of the 7th International Supercritical CO2 Power Cycles Symposium*.
[16] Pidaparti, S.R. White, C. W., Weiland, N.T. (2021). Impact of Plant Siting on Performance and Economics of Indirect Supercritical CO2 Coal Fired Power Plants. En *Turbo Expo: Power for Land, Sea, and Air*. American Society of Mechanical Engineers. p. V010T30A009.
[17] Illýes, V., Morosini, E., Doninelli, M., David, P.L., Guerif, X., Werner, A., Di Marcoberardino, G. & Manzolini, G. (2022) Design of an air-cooled condenser for CO2-based mixtures: model development, validation and heat exchange gain with internal microfin. *Proceedings of ASME Turbo Expo 2022.*
[18] Neises, T., & Turchi, C. (2019). Supercritical carbon dioxide power cycle design and configuration optimization to minimize levelized cost of energy of molten salt power towers operating at 650 C. *Solar Energy*, 181, 27-36.
[19] Thermoflow Inc, Thermoflow suite - Thermoflex software, https://www.thermoflow.com/products$_$generalpurpose.html . Retrieved October 24th 2022.
[20] Aspen plus - leading process simulator software. https://www.aspentech.com/en/products/engineering/aspen-properties. Retrieved October 24th 2022.
[21] Lemmon, E., Bell, I. H., Huber, M. & McLinden, M., NIST Standard Reference Database 23: Reference Fluid Thermodynamic and Transport Properties-REFPROP, Version 10.0, *National Institute of Standards and Technology, Standard Reference Data Program, Gaithersburg*.
[22] Shah, R. K., & Sekulic, D. P. (2003). Fundamentals of heat exchanger design. *John Wiley & Sons.*
[23] Incropera, F. P., DeWitt, D. P., Bergman, T. L., & Lavine, A. S. (1996). Fundamentals of heat and mass transfer. *New York: Wiley*.
[24] A. Cavallini, D. Del Col, L. Doretti, M. Matkovic, L. Rossetto, C. Zilio and G. Censi, "Condensation in Horizontal Smooth Tubes: A New Heat Transfer Model for Heat Exchanger Design," *Heat Transfer Engineering*, pp. 31-38, 2006.
[25] Krasnoshchekov, E. A. (1966). Experimental study of heat exchange in carbon dioxide in the supercritical range at high temperature drops. *High Temperature*, 4, 375-382.
[26] White, M. T., Bianchi, G., Chai, L., Tassou, S. A., & Sayma, A. I. (2021). Review of supercritical CO2 technologies and systems for power generation. *Applied Thermal Engineering*, 185, 116447.
[27] Kakac, S., Liu, H., & Pramuanjaroenkij, A. (2002). Heat exchangers: selection, rating, and thermal design. *CRC press*.
[28] Del Col, D., Bisetto, A., Bortolato, M., Torresin, D., & Rossetto, L. (2013). Experiments and updated model for two phase frictional pressure drop inside minichannels. *International journal of heat and mass transfer*, 67, 326-337.
[29] Brun, K., Friedman, P., & Dennis, R. (Eds.). (2017). Fundamentals and applications of supercritical carbon dioxide (sCO2) based power cycles. *Woodhead publishing.*
[30] Serth, R. W., & Lestina, T. G. (2014). Air-cooled heat exchangers. *Process Heat Transfer*, 509-553.
[31] Wilkinson, M. (2017) The Design of an Axial Flow Fan for Air-Cooled Heat Exchanger Applications, *MSc thesis, Stellenbosch University*
[32] Bruneau, P. R. P. (1994). The design of a single rotor axial flow fan for a cooling tower application. *PhD Thesis, University of Stellenbosch.*
[33] Von Backström, T.W., Buys, J.D. & Stinned, (1996). Minimization of the exit loss of a rotor-only axial fan. *Engineering Optimization+ A35*, vol. 26, no 1, p. 25-33.
[34] Meyer, C.J., Kröger, D.G. (1998). Plenum chamber flow losses in forced draught air-cooled heat exchangers. *Applied Thermal Engineering*, vol. 18, no 9-10, p. 875-893.

DOI: 10.17185/duepublico/77329

DOI: 10.17185/duepublico/77329
URN: urn:nbn:de:hbz:465-20230427-150545-4